1 # Geometrical determinant of nonlinear synaptic integration in human cortical pyramidal neurons

2

3

4 Jaeyoung Yoon[1,2,*], et al.[†]

5 [1] McGovern Institute for Brain Research, Massachusetts Institute of Technology, Cambridge, MA 02139, USA.
6 [2] Present address: F. M. Kirby Neurobiology Center, Boston Children's Hospital, & Harvard Medical School,
7 Boston, MA 02115, USA.
8 [*] Correspondence: jy.yoon@tch.harvard.edu
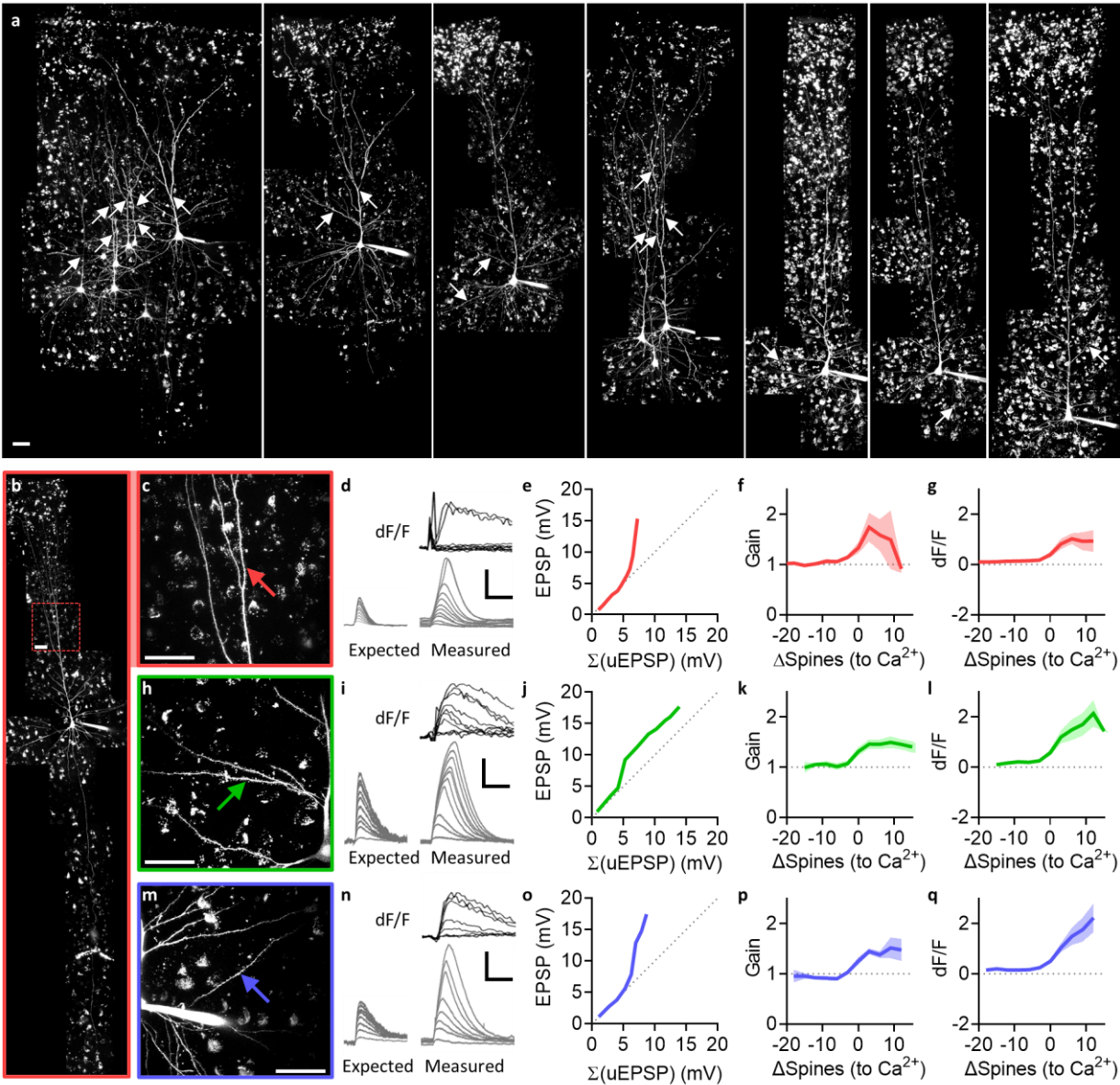9 [†] *Full author list to be determined*

10

11   **Fig. 1**

12

Figure 1. Synaptic integration at human neocortical layer 2/3 pyramidal neurons (L2/3 PN). **(a)** Representative examples of L2/3 PNs. Scale bar, 50 μm. Scale bar definitions are consistent throughout all images in all figures. Arrows indicate the center of synaptic spine clusters that were activated by 2-photon glutamate uncaging (2PGU), which typically spanned approximately 30-40 μm along the length of the branch. The high background is caused by lipofuscin aggregates on the somata of human neurons; see **Fig. 4** for comparison. **(b-c)** Representative example of an L2/3 PN, with 2PGU at the apical tuft. **(d)** Representative examples of expected EPSP (left), calculated from the arithmetic sum of unitary EPSP (uEPSP) recorded from each spine, and measured EPSP (right, bottom) recorded by quasi-simultaneous activation of spines shown in panel **c**, along with the associated fractional change in fluorescence (dF/F) obtained by intracellular calcium imaging at the parent dendrite (right, top). Scale bars, 50 ms, 5 mV, 1.0 dF/F. **(e)** Representative example of measured EPSP, plotted against the arithmetic sum of uEPSPs, from the activation of the same spines as shown in panels **b-d**. **(f)** Grouped average of synaptic gain from all apical tuft dendrites (n = 24). Gain was defined by the ratio of measured vs. expected EPSP. The number of activated spines were aligned to the threshold at which Ca^{2+} signal was first observed. **(g)** Grouped average of dF/F, associated with data shown in panel **f**. **(h-l)** Similar to panels **c-g**, but from oblique dendrites (n = 16) branching from the apical trunk. **(m-q)** Similar to panels **c-g** or **h-l**, but from basal dendrites (n = 20) branching from the soma.

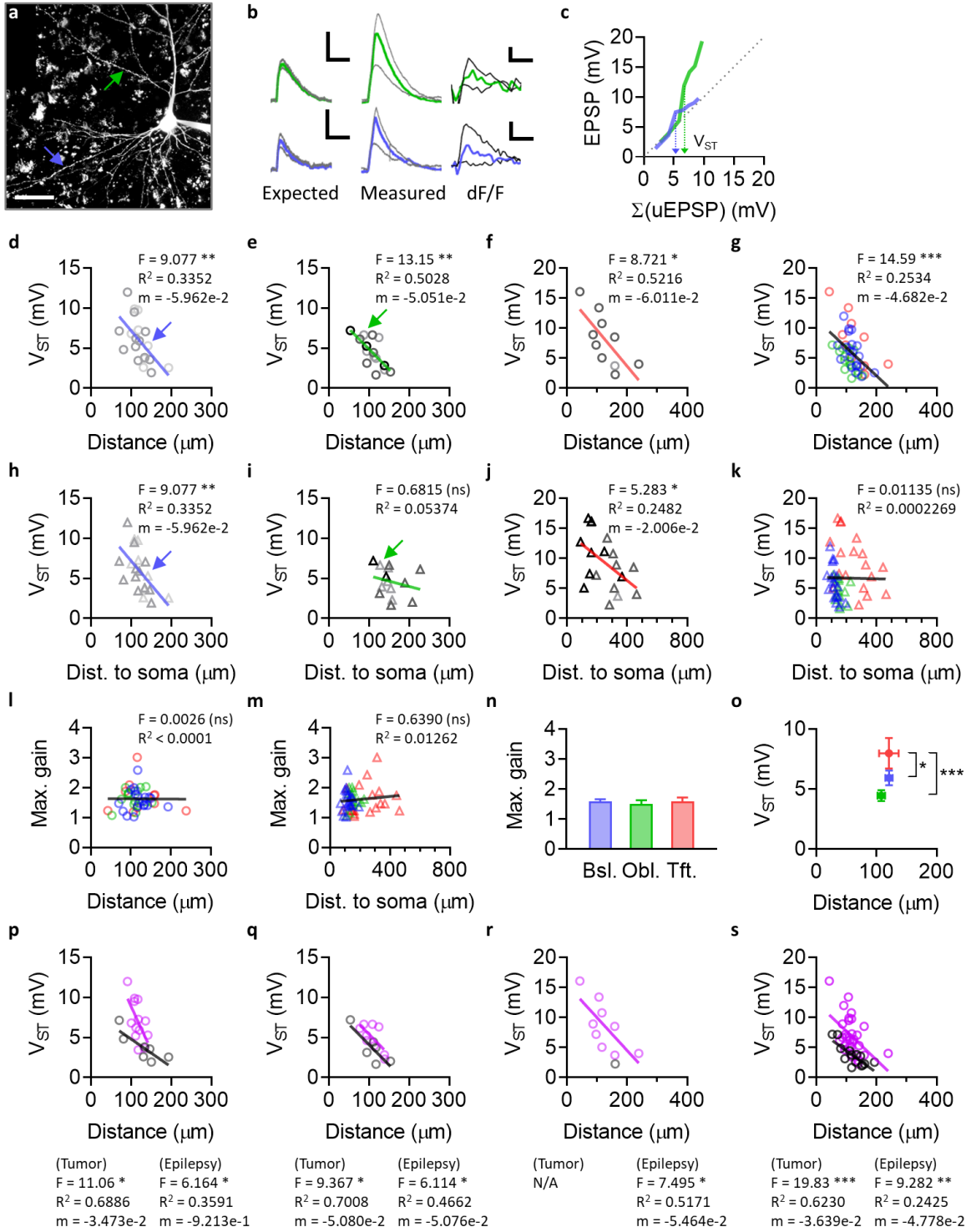**Fig. 2**

Figure 2. Somatic depolarization at supralinearity threshold (V_{ST}) is determined by synaptic distance from the apical trunk. **(a)** Representative example of a human L2/3 PN. Two different uncaging locations, one on a basal dendrite (blue) and another on an oblique dendrite (green), are indicated by arrows. Scale bar, 50 μm. **(b)** Representative traces of expected and measured EPSP, along with associated dF/F, from the branches shown in panel **a**. Scale bars, 50 ms, 5 mV, 0.5 (bottom) or 0.1 (top) dF/F. **(c)** Measured EPSP vs. expected EPSP from the sum of uEPSPs, from the same branches shown in panels **a-b**. **(d-g)** Somatic depolarization at supralinearity threshold (V_{ST}), plotted against synaptic distance. V_{ST} was defined as the expected somatic EPSP at local nonlinearity threshold indicated by the local Ca^{2+} signal; the expected EPSP from the sum of uEPSPs was used instead of the measured EPSP to determine the correct threshold irrespective of the nonlinear gain. Synaptic distance was defined as the curvilinear projected distance along the dendrite from the synapse to the nearest point on the apical trunk or the center of mass of the soma. Notably, the linear regressions in panels **d-g** had similar slopes in all groups (F = 0.06380, P = 0.9383). **(d)** V_{ST} at basal dendrites vs. distance (to soma). Shades of symbols indicate branch order (1st to 4th, darker to lighter, throughout panels **d-f**), which was not correlated with V_{ST}. **(e)** V_{ST} at oblique dendrites vs. distance (to the branch point at the apical trunk). **(f)** V_{ST} at apical tuft dendrites vs. distance to (to the branch point at the apical trunk, i.e. nexus). **(g)** Data shown in panels **d-f**, overlaid for comparison. **(h-k)** similar to panels **d-g**, but plotted instead against distance to soma; by definition of synaptic distance used in panels **d-g**, panel **h** is identical to panel **d** (for basal dendrites only). Note that in panel **j**, synapses located at the nexus are also included, whereas they were excluded from panel **f** due to having zero synaptic distance as defined. **(l)** Maximum gain vs. synaptic distance, to the nearest point on the apical trunk or the soma. **(m)** Maximum gain vs. distance to soma. **(n)** Maximum gain at basal, oblique, and tuft dendrites. **(o)** Average V_{ST} at basal, oblique, and tuft dendrites. **(p-s)** Same data as in panels **d-g**, but grouped separately by tumor (black) or epilepsy (purple). Neurons from the cortex associated with epilepsy had a tendency of higher V_{ST} for a given synaptic distance, compared to those from tumor tissue.
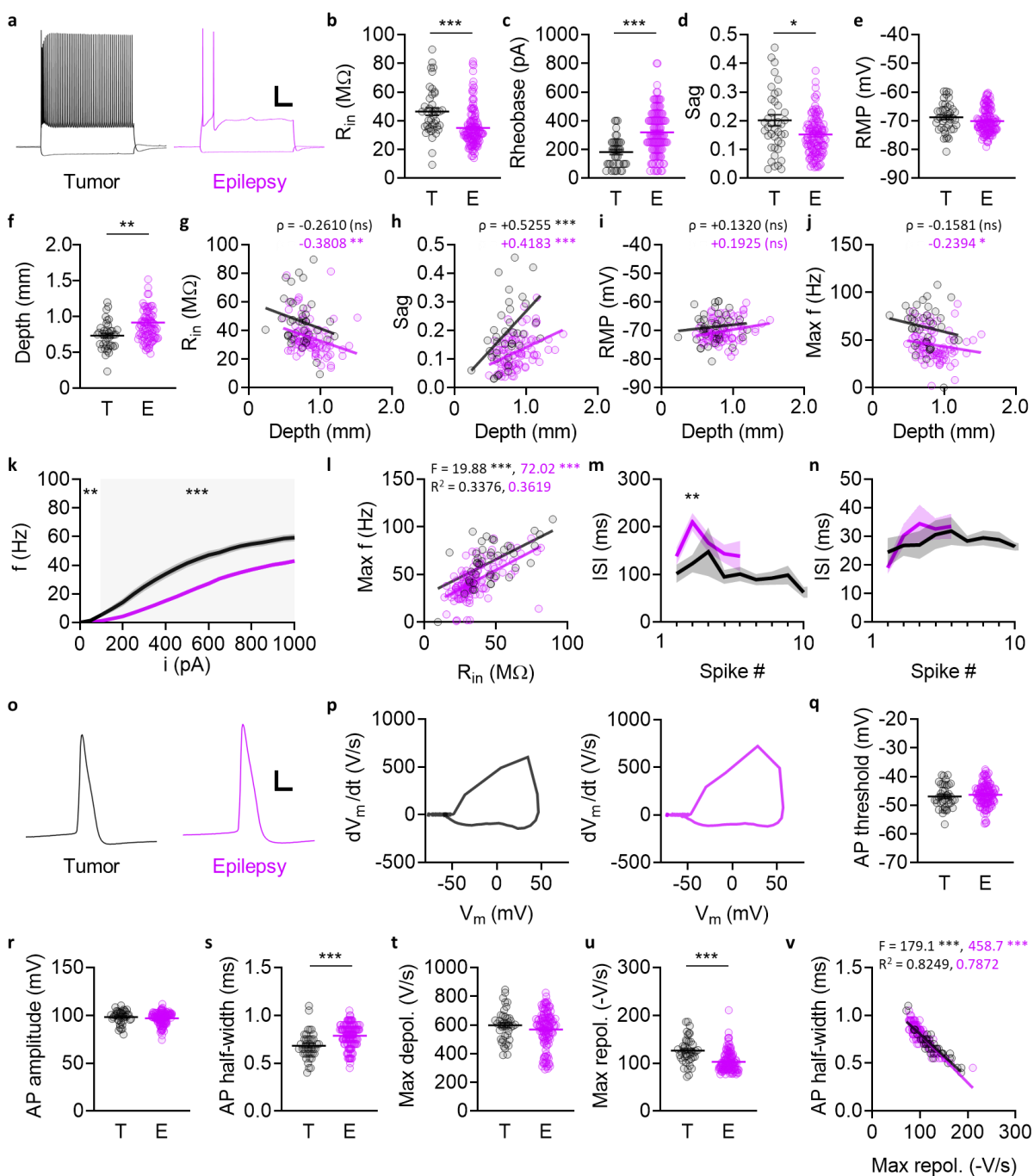
Fig. 3

Figure 3. Intrinsic membrane properties of human L2/3 PN, from tumor (black) or epilepsy (purple). For more detailed patient and tissue information, see **Table 1**. Note that tissue from both tumor and epilepsy patients originated from areas determined to be nonpathological, but removed as part of the surgical procedure. **(a)** Representative traces of membrane potential responses to somatic step current injection (-250 pA, +1000 pA). Scale bar, 20 mV, 200 ms. The example to the right was taken from the same cell as in **Fig. 1b**. **(b)** Input resistance (R_{in}). See methods for R_{in} calculation. **(c)** Rheobase, with current step resolution of 50 pA. **(d)** Sag ratio. See methods for the definition of sag ratio. **(e)** Resting membrane potential (RMP). **(f)** Sampling bias in the cortical depths of recorded L2/3 PNs included in the current study. Cortical depth of a recorded cell was defined as the linear distance between the pial surface and the soma, extrapolated from the line connecting the soma and the nexus. The depth of one outlier in the tumor group (235 μm) and its identity as an L2/3 PN was verified with the whole-cell 2-photon image of the cell along with neighboring L2/3 PNs deeper within the cortex, all of which had dendritic arbors that were intact up to the pia mater and in plane. **(g-j)** Intrinsic membrane properties, plotted against cortical depth. **(g)** R_{in}. **(h)** Sag ratio. **(i)** RMP. **(j)** Peak firing rate. **(k)** Firing frequency in response to somatic current injection. L2/3 PN firing frequency was significantly lower in epilepsy compared to tumor ($P < 0.001$ each for all $i \geq 100$ (pA), $P < 0.01$ for $i = 50$ (pA)). **(l)** Peak firing rate, plotted against R_{in}. **(m)** Inter-spike interval (ISI) at rheobase. **(n)** ISI at 2*rheobase. **(o)** Representative traces of single action potentials (AP) from human L2/3 PNs. For each cell, the first action potential generated at rheobase was taken for analysis. Scale bar, 20 mV, 1 ms. The example to the right was taken from the same cell as in **Fig. 2a**. **(p)** Example AP waveforms presented as dV/dt plots, calculated from the same traces as in panel **o**. **(q)** AP threshold. AP threshold was defined as the V_m at which dV/dt crossed 10 (V/s). **(r)** AP amplitude (RMP to AP peak). **(s)** AP half-width. **(t)** Maximum rate of depolarization. **(u)** Maximum rate of repolarization. **(v)** AP half-width plotted against the maximum rate of repolarization.
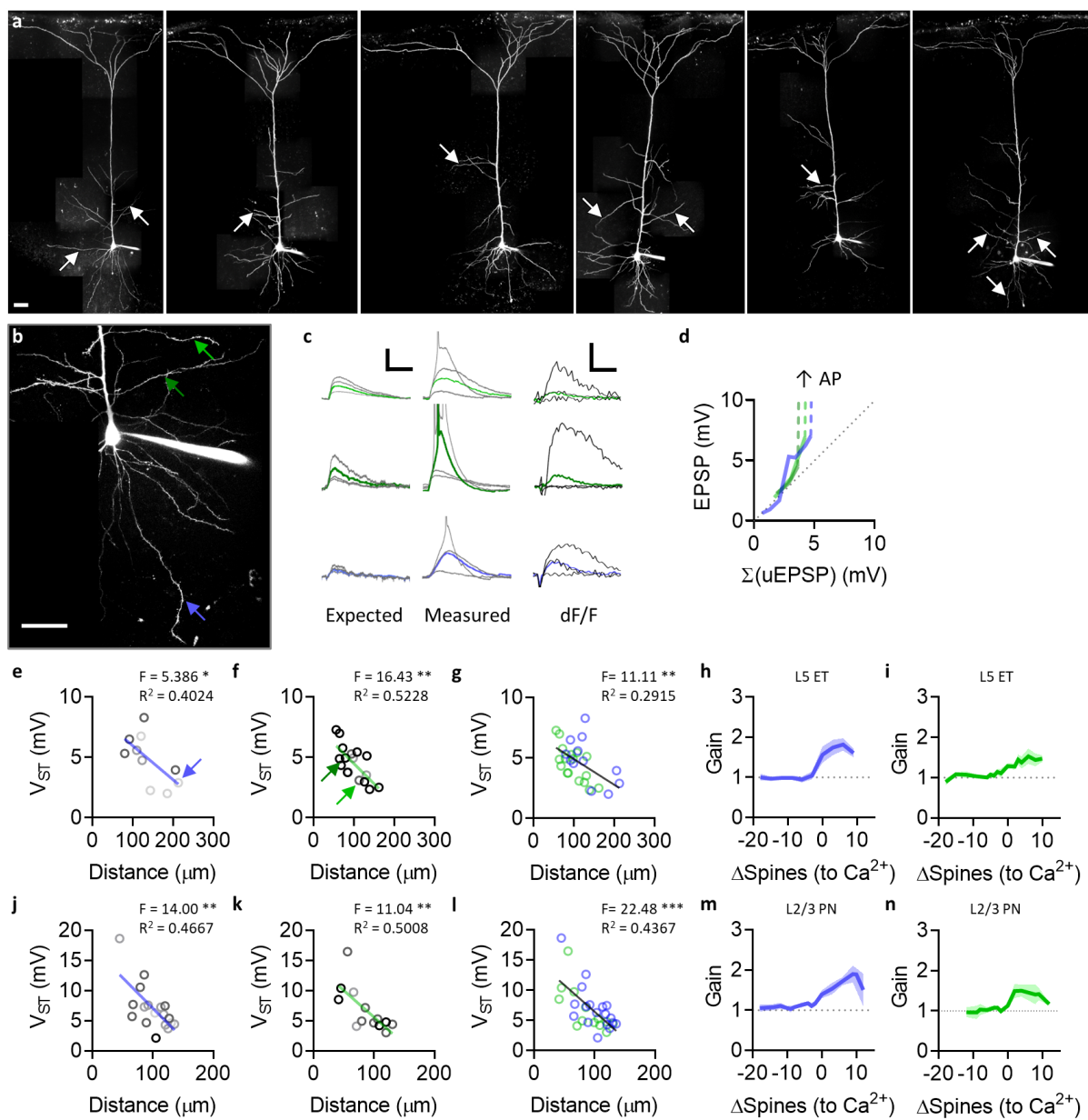
Fig. 4

Figure 4. Somatic depolarization at supralinearity threshold (V_{ST}) is determined analogously by synaptic distance from the apical trunk in rodents as well as in humans, and for both supragranular and infragranular cortical pyramidal neurons. **(a)** Representative examples of rat L5 extratelencephalic (ET) PNs, from the temporal association area (TeA). Arrows indicate uncaging locations. Scale bar, 50 μm. Compare with **Fig. 1** for the difference in background caused by lipofuscin in the human cortex. **(b)** Representative example of a L5 ET PN, with three different uncaging locations; one on a basal dendrite, and two on separate oblique dendrites. **(c)** Representative traces from the uncaging locations shown in panel a. Scale bars, 50 ms, 5 mV, 0.5 dF/F. **(d)** Measured EPSP vs. expected EPSP from the sum of uEPSPs, from the branches shown in panels **b-c**. **(e-g)** V_{ST} vs. synaptic distance as defined in **Fig. 2**, in rat L5 ET. The slopes of the regressions in panels **e** and **f** were not significantly different (F = 0.5381, P = 0.4700). **(e)** Basal dendrites. **(f)** Oblique dendrites. **(g)** Data shown in panels **e-f**, overlaid for comparison. **(h)** Synaptic gain, at basal dendrites shown in panel **e**. **(i)** Synaptic gain, at oblique dendrites shown in panel **f**. **(j-n)** Similar to panels **e-g**, but from rat L2/3 PNs instead of L5 ET. The slopes of the regressions in panels **j** and **k** were not significantly different (F = 0.1038, P = 0.7498). **(j)** Basal dendrites. **(k)** Oblique dendrites. **(l)** Data shown in panels **j-k**, overlaid for comparison. **(m)** Synaptic gain, at basal dendrites shown in panel **j**. **(n)** Synaptic gain, at oblique dendrites shown in panel **k**.

113 **Table 1** (redacted for preview)

ID	Age	Sex	Area	Hemi.	Medications (AED)	Diagnosis	n (cells/humans)
-	-	-	-	-	-	-	-
-	-	-	-	-	-	-	-
-	-	-	-	-	-	-	-
-	-	-	-	-	-	-	-
-	-	-	-	-	-	-	-
-	-	-	-	-	-	-	-
-	-	-	-	-	-	-	-
-	-	-	-	-	-	-	-
-	-	-	-	-	-	-	-
-	-	-	-	-	-	-	-
-	-	-	-	-	-	-	-
-	-	-	-	-	-	-	-
-	-	-	-	-	-	-	-
-	-	-	-	-	-	-	-
-	-	-	-	-	-	-	-
-	-	-	-	-	-	-	-
-	-	-	-	-	-	-	-
-	-	-	-	-	-	-	-
-	-	-	-	-	-	-	-
-	-	-	-	-	-	-	-
-	-	-	-	-	-	-	-
-	-	-	-	-	-	-	-
						(Tumor)	43/5
						(Epilepsy)	119/17
						(Total)	162/22

-

114 **Table 1.** Patient and tissue information. (redacted for preview)

115